



## T-MATRIX COMPUTATIONS OF LIGHT SCATTERING BY NONSPHERICAL PARTICLES: A REVIEW

MICHAEL I. MISHCHENKO,<sup>a†</sup> LARRY D. TRAVIS,<sup>a</sup> and  
 DANIEL W. MACKOWSKI<sup>b</sup>

<sup>a</sup>NASA Goddard Institute for Space Studies, 2880 Broadway, New York, NY 10025 and

<sup>b</sup>Department of Mechanical Engineering, Auburn University, Auburn, AL 36849-5341, U.S.A.

**Abstract**—We review the current status of Waterman's *T*-matrix approach which is one of the most powerful and widely used tools for accurately computing light scattering by nonspherical particles, both single and composite, based on directly solving Maxwell's equations. Specifically, we discuss the analytical method for computing orientationally-averaged light-scattering characteristics for ensembles of nonspherical particles, the methods for overcoming the numerical instability in calculating the *T* matrix for single nonspherical particles with large size parameters and/or extreme geometries, and the superposition approach for computing light scattering by composite/aggregated particles. Our discussion is accompanied by multiple numerical examples demonstrating the capabilities of the *T*-matrix approach and showing effects of nonsphericity of simple convex particles (spheroids) on light scattering.

### 1. INTRODUCTION

Accurate information about light scattering properties of small nonspherical particles is important in many fields of science and engineering, such as atmospheric optics, oceanography, radar meteorology, aerosol science and technology, electrical engineering, astrophysics, colloidal chemistry, biophysics, and particle sizing. Often one has to deal with particles which are neither much smaller nor much larger than the wavelength of the incident radiation. In this so-called resonance region of particle size parameters, the Rayleigh and the geometric optics approximations are inapplicable,<sup>1–3</sup> and numerical methods for computing nonspherical scattering must be based on directly solving Maxwell's equations. Reviews of such methods can be found, e.g., in Refs. 4–11.

At present, Waterman's *T*-matrix approach<sup>5,12–18</sup> is one of the most powerful and widely used tools for rigorously computing light scattering by resonance nonspherical particles, both single and aggregated, and favorably compares with other frequently used methods such as the discrete dipole approximation/volume integral equation formulation<sup>19–21</sup> and the separation of variables method for spheroids.<sup>22,23</sup> Because of its superior efficiency, the *T*-matrix method is the only technique that has been used in systematic studies of resonance nonspherical scattering based on calculations for hundreds and thousands of different particles in random orientation. Moreover, recent improvements have made it applicable to particles with size parameters well exceeding 50, and, therefore, suitable for checking the accuracy of the geometric optics approximation at lower frequencies.

In this paper we review the current status of the *T*-matrix approach with emphasis on what makes it especially attractive mathematically and efficient and powerful numerically. The following section gives an overview of the *T*-matrix approach in application to an arbitrary nonspherical particle, either single or composite, discusses properties of special functions which play a key role in the *T*-matrix mathematical formulation, and describes an efficient analytical method for computing orientationally-averaged light-scattering characteristics for ensembles of nonspherical particles. In Sec. 3 we briefly discuss the basic scheme for computing the *T*-matrix for single scatterers (homogeneous or layered) and describe the methods for handling the numerical instability in calculating the *T* matrix for particles that are large compared with a wavelength

<sup>†</sup>To whom all correspondence should be addressed.

and/or have extreme geometries such as highly elongated or highly flattened spheroids. In Sec. 4, the superposition  $T$ -matrix approach for computing light scattering by composite/aggregated particles is summarized. In Sec. 5 we briefly review practical applications of the  $T$ -matrix approach and present the results of extensive numerical computations demonstrating the capabilities of the  $T$ -matrix approach and showing effects of nonsphericity of simple convex particles (spheroids) on light scattering.

## 2. $T$ -MATRIX ANSATZ AND ANALYTICAL AVERAGING OVER PARTICLE ORIENTATIONS

To describe the scattering of light by an arbitrary nonspherical particle, we use a right-handed spherical coordinate system with orientation fixed in space, having its origin inside the particle. Consider a plane electromagnetic wave incident in the direction specified by a unit vector  $\mathbf{n}_{\text{inc}}$  or, equivalently, by a couple  $(\vartheta_{\text{inc}}, \varphi_{\text{inc}})$ , and given by

$$\mathbf{E}^{\text{inc}}(\mathbf{R}) = \mathbf{E}^{\text{inc}} \exp(ik \mathbf{n}_{\text{inc}} \mathbf{R}) = (E_{\vartheta}^{\text{inc}} \mathbf{\vartheta}_{\text{inc}} + E_{\varphi}^{\text{inc}} \mathbf{\varphi}_{\text{inc}}) \exp(ik \mathbf{n}_{\text{inc}} \mathbf{R}), \quad (1)$$

where  $i = (-1)^{1/2}$ ,  $k = 2\pi/\lambda$  is the free-space wavenumber for free-space wavelength  $\lambda$ ,  $\mathbf{R}$  is the radius vector with its origin at the origin of the coordinate system, and  $\mathbf{\vartheta}_{\text{inc}}$  and  $\mathbf{\varphi}_{\text{inc}}$  are the unit vectors in the  $\vartheta$ - and  $\varphi$ -directions such that  $\mathbf{n}_{\text{inc}} = \mathbf{\vartheta}_{\text{inc}} \times \mathbf{\varphi}_{\text{inc}}$ . The time factor  $\exp(-i\omega t)$  is assumed and is suppressed throughout the paper. In the far-field region ( $kR \gg 1$ ), the scattered wave becomes spherical and is given by

$$\mathbf{E}^{\text{sca}}(\mathbf{R}) = E_{\vartheta}^{\text{sca}}(R, \mathbf{n}_{\text{sca}}) \mathbf{\vartheta}_{\text{sca}} + E_{\varphi}^{\text{sca}}(R, \mathbf{n}_{\text{sca}}) \mathbf{\varphi}_{\text{sca}}, \quad \mathbf{n}_{\text{sca}} = \mathbf{R}/R, \quad kR \gg 1, \quad (2)$$

$$\mathbf{R} \mathbf{E}^{\text{sca}}(\mathbf{R}) = 0, \quad (3)$$

$$\begin{bmatrix} E_{\vartheta}^{\text{sca}} \\ E_{\varphi}^{\text{sca}} \end{bmatrix} = \frac{\exp(ikR)}{R} \mathbf{S}(\mathbf{n}_{\text{sca}}, \mathbf{n}_{\text{inc}}) \begin{bmatrix} E_{\vartheta}^{\text{inc}} \\ E_{\varphi}^{\text{inc}} \end{bmatrix}, \quad (4)$$

where  $\mathbf{S}$  is a  $(2 \times 2)$  amplitude scattering matrix which linearly transforms the electric vector components of the incident wave into the electric vector components of the scattered wave. The amplitude scattering matrix depends on the directions of incidence and scattering as well as on the size, morphology, and composition of the scattering particle and on its orientation with respect to the reference frame. The amplitude scattering matrix is the primary quantity that defines the scattering law. If known, it enables one to compute any other light scattering characteristic of the particle.

In the framework of the  $T$ -matrix approach, the incident and scattered fields are expressed in vector spherical functions  $\mathbf{M}_{mn}$  and  $\mathbf{N}_{mn}$  as follows:<sup>17,24</sup>

$$\mathbf{E}^{\text{inc}}(\mathbf{R}) = \sum_{n=1}^{\infty} \sum_{m=-n}^n [a_{mn} \text{Rg} \mathbf{M}_{mn}(k\mathbf{R}) + b_{mn} \text{Rg} \mathbf{N}_{mn}(k\mathbf{R})], \quad (5)$$

$$\mathbf{E}^{\text{sca}}(\mathbf{R}) = \sum_{n=1}^{\infty} \sum_{m=-n}^n [p_{mn} \mathbf{M}_{mn}(k\mathbf{R}) + q_{mn} \mathbf{N}_{mn}(k\mathbf{R})], \quad R > r_0, \quad (6)$$

where

$$\mathbf{M}_{mn}(k\mathbf{R}) = (-1)^m d_n h_n^{(1)}(kR) \mathbf{C}_{mn}(\vartheta) \exp(im\varphi), \quad (7)$$

$$\mathbf{N}_{mn}(k\mathbf{R}) = (-1)^m d_n \left\{ \frac{n(n+1)}{kR} h_n^{(1)}(kR) \mathbf{P}_{mn}(\vartheta) + \frac{1}{kR} [kR h_n^{(1)}(kR)]' \mathbf{B}_{mn}(\vartheta) \right\} \exp(im\varphi), \quad (8)$$

$$\mathbf{B}_{mn}(\vartheta) = \vartheta \frac{d}{d\vartheta} d_{0m}^n(\vartheta) + \varphi \frac{im}{\sin \vartheta} d_{0m}^n(\vartheta), \quad (9)$$

$$\mathbf{C}_{mn}(\vartheta) = \vartheta \frac{im}{\sin \vartheta} d_{0m}^n(\vartheta) - \varphi \frac{d}{d\vartheta} d_{0m}^n(\vartheta), \quad (10)$$

$$\mathbf{P}_{mn}(\vartheta) = \mathbf{R} d_{0m}^n(\vartheta)/R, \quad (11)$$

$$d_n = \left[ \frac{2n+1}{4\pi n(n+1)} \right]^{1/2}, \quad (12)$$

$r_0$  is the radius of a circumscribing sphere of the scattering particle, and  $d_{lm}^n(\vartheta)$  are Wigner  $d$ -functions<sup>25</sup> given by

$$d_{lm}^n(\vartheta) = A_{lm}^n (1 - \cos \vartheta)^{(l-m)/2} (1 + \cos \vartheta)^{-(l+m)/2} \frac{d^{n-m}}{(d \cos \vartheta)^{n-m}} [(1 - \cos \vartheta)^{n-l} (1 + \cos \vartheta)^{n+l}] \quad (13)$$

for  $n \geq n_* = \max(|l|, |m|)$  and by

$$d_{lm}^n(\vartheta) = 0 \quad (14)$$

for  $n < n_*$ . In Eq. (13),

$$A_{lm}^n = \frac{(-1)^{n-m}}{2^n} \left[ \frac{(n+m)!}{(n-l)!(n+l)!(n-m)!} \right]^{1/2}. \quad (15)$$

Convenient recurrence formulas for computing Wigner  $d$  functions are given in Ref. 25. The expressions for the functions  $\text{Rg } \mathbf{M}_{mn}$  and  $\text{Rg } \mathbf{N}_{mn}$  can be obtained from Eqs. (7) and (8) by replacing spherical Hankel functions  $h_n^{(1)}$  by spherical Bessel functions  $j_n$ . The expansion coefficients of the plane incident wave are<sup>17</sup>

$$a_{mn} = 4\pi (-1)^m i^n d_n \mathbf{C}_{mn}^*(\vartheta_{\text{inc}}) \mathbf{E}^{\text{inc}} \exp(-im\varphi_{\text{inc}}), \quad (16)$$

$$b_{mn} = 4\pi (-1)^m i^{n-1} d_n \mathbf{B}_{mn}^*(\vartheta_{\text{inc}}) \mathbf{E}^{\text{inc}} \exp(-im\varphi_{\text{inc}}), \quad (17)$$

where an asterisk indicates complex conjugation.

Owing to the linearity of Maxwell's equations and boundary conditions, the relation between the scattered field coefficients  $p_{mn}$  and  $q_{mn}$  on one hand and the incident field coefficients  $a_{mn}$  and  $b_{mn}$  on the other hand is linear and is given by a transition matrix (or  $T$  matrix)  $\mathbf{T}$  as follows:<sup>14,17</sup>

$$p_{mn} = \sum_{n'=1}^{\infty} \sum_{m'=-n'}^{n'} [T_{mnm'n'}^{11} a_{m'n'} + T_{mnm'n'}^{12} b_{m'n'}], \quad (18)$$

$$q_{mn} = \sum_{n'=1}^{\infty} \sum_{m'=-n'}^{n'} [T_{mnm'n'}^{21} a_{m'n'} + T_{mnm'n'}^{22} b_{m'n'}]. \quad (19)$$

In a compact matrix notation, Eqs. (18) and (19) can be rewritten as

$$\begin{bmatrix} \mathbf{p} \\ \mathbf{q} \end{bmatrix} = \mathbf{T} \begin{bmatrix} \mathbf{a} \\ \mathbf{b} \end{bmatrix} = \begin{bmatrix} \mathbf{T}^{11} & \mathbf{T}^{12} \\ \mathbf{T}^{21} & \mathbf{T}^{22} \end{bmatrix} \begin{bmatrix} \mathbf{a} \\ \mathbf{b} \end{bmatrix}. \quad (20)$$

Equation (20) is a cornerstone of the  $T$ -matrix formulation. If the  $T$  matrix for a given scatterer is known, Eqs. (20), (16), (17), (6), and (4) can be used to compute the scattered field and, thus, the amplitude scattering matrix. Specifically, making use of the large argument approximation for spherical Hankel functions,

$$h_n^{(1)}(kR) \simeq \frac{(-2)^{n+1} \exp(ikR)}{kR}, \quad kR \gg n^2, \quad (21)$$

we have in dyadic notation<sup>17</sup>

$$\begin{aligned} \mathbf{S}(\mathbf{n}_{\text{sca}}, \mathbf{n}_{\text{inc}}) &= \frac{4\pi}{k} \sum_{nm'n'} i^{n'-n-1} (-1)^{m+m'} d_n d_{n'} \exp[i(m\varphi_{\text{sca}} - m'\varphi_{\text{inc}})] \\ &\times \{ [T_{nmn'm'}^{11} \mathbf{C}_{mn}(\vartheta_{\text{sca}}) + T_{nmn'm'}^{21} i \mathbf{B}_{mn}(\vartheta_{\text{sca}})] \mathbf{C}_{m'n'}^*(\vartheta_{\text{inc}}) \\ &+ [T_{nmn'm'}^{12} \mathbf{C}_{mn}(\vartheta_{\text{sca}}) + T_{nmn'm'}^{22} i \mathbf{B}_{mn}(\vartheta_{\text{sca}})] \mathbf{B}_{m'n'}^*(\vartheta_{\text{inc}}) / i \}. \end{aligned} \quad (22)$$

A fundamental feature of the  $T$ -matrix approach is that the elements of the  $T$  matrix are independent of the incident and scattered fields and depend only on the shape, size parameter, and refractive index of the scattering particle as well as on its orientation with respect to the coordinate system. Consequently, the  $T$  matrix need be computed only once and then can be used in computations for any directions of light incidence and scattering.

An additional crucial advantage of the  $T$ -matrix approach is analyticity of its mathematical formulation. Indeed, mathematical properties of all special functions used are well known and can be used to derive general properties of the  $T$  matrix and to analytically average light-scattering

properties over particle orientations. The latter feature is of particular significance since, in most natural circumstances, particles are distributed over a range of orientations rather than being perfectly aligned.

We begin with the derivation of the rotation transformation rule for the  $T$  matrix. Consider two arbitrary coordinate systems having a common origin inside the scattering particle and let  $\alpha$ ,  $\beta$ , and  $\gamma$  be the Euler angles of rotation that transform coordinate system 2 into coordinate system 1.<sup>25</sup> Let also  $(kR, \vartheta_1, \varphi_1)$  and  $(kR, \vartheta_2, \varphi_2)$  be the spherical coordinates of the same radius vector  $kR$  in the two coordinate systems. We then have<sup>25</sup>

$$\mathbf{M}_{mm}(kR, \vartheta_1, \varphi_1) = \sum_{m'=-n}^n D_{m'm}^n(\alpha, \beta, \gamma) \mathbf{M}_{m'n}(kR, \vartheta_2, \varphi_2), \quad (23)$$

where

$$D_{m'm}^n(\alpha, \beta, \gamma) = \exp(-im'\alpha) d_{m'm}^n(\beta) \exp(-im\gamma) \quad (24)$$

are Wigner  $D$  functions. The corresponding inverse relation is

$$\mathbf{M}_{mm}(kR, \vartheta_2, \varphi_2) = \sum_{m'=-n}^n [D_{mm'}^n(\alpha, \beta, \gamma)]^* \mathbf{M}_{m'n}(kR, \vartheta_1, \varphi_1). \quad (25)$$

Similar expansions hold for the functions  $\mathbf{N}_{mm}$ ,  $\text{Rg } \mathbf{M}_{mm}$ , and  $\text{Rg } \mathbf{N}_{mm}$ . Let  ${}^1\mathbf{T}$  and  ${}^2\mathbf{T}$  be the  $T$  matrices of a particle with respect to the coordinate systems 1 and 2, respectively. Taking into account Eqs. (5), (6), (18), (19), (23), and (25), we derive<sup>17,26</sup>

$${}^2T_{mm'n'}^{ij} = \sum_{m_1=-n}^n \sum_{m_2=-n'}^{n'} [D_{m'm_2}^{n'}(\alpha, \beta, \gamma)]^* {}^1T_{m_1m_2n}^{ij} D_{mm_1}^n(\alpha, \beta, \gamma), \quad i, j = 1, 2. \quad (26)$$

If we now assume that the  $T$  matrix  ${}^1\mathbf{T}$  is already known, then we can think of the Euler angles of rotation,  $\alpha$ ,  $\beta$ , and  $\gamma$  as specifying the orientation of the particle with respect to the coordinate system 2 and can use Eq. (26) to compute the corresponding  ${}^2\mathbf{T}$  matrix. This can be done for any  $\alpha$ ,  $\beta$ , and  $\gamma$ , and, therefore, Eq. (26), in conjunction with Eq. (22), is ideally suited for computing orientationally averaged light scattering in the coordinate system 2 using a single precalculated  ${}^1\mathbf{T}$  matrix.<sup>17,26</sup>

Note that the choice of the coordinate system 1 to compute the  $T$  matrix can be arbitrary for irregularly shaped particles. However, for particles with special symmetries a proper choice of the coordinate system can substantially simplify the problem. This explains why the coordinate system 1 is often called the natural coordinate system of the scatterer. For example, for rotationally symmetric particles, it is advantageous to direct the  $z$  axis of the natural coordinate system along the axis of particle symmetry. In this case, the amplitude scattering matrix must obey the symmetry relations<sup>1</sup>

$$\mathbf{S}(\mathbf{n}_{\text{sca}}, \mathbf{n}_{\text{inc}}) = \mathbf{S}(\vartheta_{\text{sca}}, \vartheta_{\text{inc}}, \varphi_{\text{sca}} - \varphi_{\text{inc}}), \quad (27)$$

$$\mathbf{S}(\vartheta_{\text{sca}}, \vartheta_{\text{inc}}, \varphi_{\text{sca}} - \varphi_{\text{inc}}) = \mathbf{Q} \mathbf{S}(\vartheta_{\text{sca}}, \vartheta_{\text{inc}}, \varphi_{\text{inc}} - \varphi_{\text{sca}}) \mathbf{Q}, \quad (28)$$

where

$$\mathbf{Q} = \text{diag}[1, -1]. \quad (29)$$

As a result, the  ${}^1\mathbf{T}$  matrix in the natural coordinate system becomes diagonal with respect to the azimuthal indices  $m$  and  $m'$  and we have

$${}^1T_{mm'n'}^{ij} = \delta_{mm'} {}^1T_{mmn}^{ij}, \quad (30)$$

$${}^1T_{mmn}^{ij} = (-1)^{i+j} {}^1T_{-m, -n}^{ij}. \quad (31)$$

The  $T$  matrix becomes especially simple for spherical particles, in which case we have for any coordinate system:

$$T_{mm'n'}^{11} = -\delta_{nn'} b_n, \quad (32)$$

$$T_{mm'n'}^{22} = -\delta_{nn'} a_n, \quad (33)$$

$$T_{mm'n'}^{12} = T_{mm'n'}^{21} \equiv 0, \quad (34)$$

where  $a_n$  and  $b_n$  are the well known Mie coefficients.<sup>2</sup> Moreover, in the case of spherical particle shape all formulas of the *T*-matrix approach become identical to the corresponding formulas of Mie theory. Therefore, the *T*-matrix approach can be considered an extension of Mie theory to nonspherical particles.

Using Eq. (22) and the general reciprocity relation for the amplitude scattering matrix,<sup>27,28</sup>

$$S(-\mathbf{n}_{\text{inc}}, -\mathbf{n}_{\text{sca}}) = \mathbf{Q} S^T(\mathbf{n}_{\text{sca}}, \mathbf{n}_{\text{inc}}) \mathbf{Q}, \quad (35)$$

where *T* stands for matrix transpose, we derive the following general symmetry relation for the *T* matrix elements:

$$T_{mm'n'}^{ij} = (-1)^{m+m'} T_{-m'-n'-mn}^{ji}. \quad (36)$$

This relation can be used in practice for checking the numerical accuracy of computing the *T* matrix. Also, employing Eq. (26) and the unitarity property of Wigner *D* functions,<sup>25</sup>

$$\sum_{m'=-n}^n [D_{m'm}^n(\alpha, \beta, \gamma)]^* D_{m'm}^n(\alpha, \beta, \gamma) = \delta_{mm'}, \quad (37)$$

we obtain the following two general invariants with respect to rotations of the coordinate system:<sup>29,30</sup>

$$\sum_{m=-n}^n {}^1T_{nnmm}^{ij} = \sum_{m=-n}^n {}^2T_{nnmm}^{ij}, \quad (38)$$

$$\sum_{m=-n}^n \sum_{m'=-n'}^{n'} |{}^1T_{mm'n'n'}^{ij}|^2 = \sum_{m=-n}^n \sum_{m'=-n'}^{n'} |{}^2T_{mm'n'n'}^{ij}|^2. \quad (39)$$

Equation (26) is the basis of analytical procedures for averaging light scattering characteristics over particle orientations. In the simplest and practically most important case of randomly oriented particles, the orientation distribution function  $P(\alpha, \beta, \gamma)$  is equal to  $(8\pi^2)^{-1}$ . Therefore, using Eq. (26) and the orthogonality relation for Wigner *D* functions<sup>25</sup>

$$\int_0^{2\pi} d\alpha \int_0^\pi d\beta \sin \beta \int_0^{2\pi} d\gamma D_{mm'}^n(\alpha, \beta, \gamma) [D_{m_1m_1'}^{n'}(\alpha, \beta, \gamma)]^* = \frac{8\pi^2}{2n+1} \delta_{nn'} \delta_{mm_1} \delta_{m'm_1'}, \quad (40)$$

we derive for the orientationally averaged *T* matrix<sup>31</sup>

$$\langle {}^2T_{mm'n'n'}^{ij} \rangle = \frac{1}{2n+1} \delta_{mm'} \delta_{nn'} \sum_{m_1=-n}^n {}^1T_{m_1nm_1n}^{ij}, \quad i, j = 1, 2. \quad (41)$$

As a result, we obtain the following general formula for the extinction cross section of randomly oriented particles<sup>17,31</sup>

$$\begin{aligned} \langle C_{\text{ext}} \rangle &= \frac{2\pi}{k} \text{Im}[\langle S_{gg}(\mathbf{n}, \mathbf{n}) \rangle + \langle S_{\varphi\varphi}(\mathbf{n}, \mathbf{n}) \rangle] \\ &= -\frac{2\pi}{k^2} \text{Re} \sum_{n=1}^{\infty} \sum_{m=-n}^n [{}^1T_{nnmm}^{11} + {}^1T_{nnmm}^{22}]. \end{aligned} \quad (42)$$

[Note that an analogous but less simple formula was derived by Borghese et al.<sup>32</sup>] Thus the average extinction cross section is proportional to the real part of the sum of the diagonal elements of the *T* matrix computed in an arbitrarily chosen reference frame. An equally simple formula can be derived for the scattering cross section of randomly oriented particles:<sup>24,29</sup>

$$\langle C_{\text{sca}} \rangle = \frac{2\pi}{k^2} \sum_{n=1}^{\infty} \sum_{n'=1}^{\infty} \sum_{m=-n}^n \sum_{m'=-n'}^{n'} \sum_{i=1}^2 \sum_{j=1}^2 |{}^1T_{mm'n'n'}^{ij}|^2. \quad (43)$$

The orientationally averaged extinction and scattering cross sections must be invariant with respect to the choice of the coordinate system, and, indeed, this invariance follows from Eqs. (38), (39), (42), and (43).

For nonabsorbing particles, the orientationally averaged extinction cross section must be equal to the orientationally averaged scattering cross section. Therefore, the  $T$  matrix elements for nonabsorbing particles must satisfy the condition [cf. Eqs. (42) and (43)]

$$-\operatorname{Re} \sum_{n=1}^{\infty} \sum_{m=-n}^n [T_{nnnn}^{11} + T_{nnnn}^{22}] = \sum_{n=1}^{\infty} \sum_{n'=1}^{\infty} \sum_{m=-n}^n \sum_{m'=-n'}^{n'} \sum_{i=1}^2 \sum_{j=1}^2 |T_{nnmm'}^{ij}|^2. \quad (44)$$

Applying the principle of conservation of energy to nonabsorbing particles in a fixed orientation, one can derive the unitarity condition<sup>17</sup>

$$\mathbf{T}^+ \mathbf{T} = -\frac{1}{2} \{\mathbf{T}^+ + \mathbf{T}\}, \quad (45)$$

where the superscript  $+$  denotes Hermitian conjugate. Equations (44) and (45) can be used as simple numerical checks in  $T$ -matrix computations for lossless scatterers.

The Stokes scattering matrix transforms the Stokes parameters of the incident light into those of the scattered light.<sup>1,2</sup> In the standard  $(I, Q, U, V)$ -representation of polarization, the scattering matrix for randomly oriented particles with a plane of symmetry has the well-known block-diagonal form<sup>1,2</sup>

$$\mathbf{F}(\Theta) = \begin{bmatrix} a_1(\Theta) & b_1(\Theta) & 0 & 0 \\ b_1(\Theta) & a_2(\Theta) & 0 & 0 \\ 0 & 0 & a_3(\Theta) & b_2(\Theta) \\ 0 & 0 & -b_2(\Theta) & a_4(\Theta) \end{bmatrix}, \quad (46)$$

where  $\Theta \in [0, \pi]$  is the scattering angle (i.e., the angle between the incident and scattered beams), and the  $(1, 1)$ -element (i.e., the phase function) is assumed to be normalized as

$$\frac{1}{2} \int_0^\pi d\Theta \sin \Theta a_1(\Theta) = 1. \quad (47)$$

Computation of the elements of this matrix requires orientational averaging of products of the amplitude matrix elements given by Eq. (22). This problem has been studied by Mishchenko<sup>24</sup> for the case of rotationally symmetric particles and by Khlebtsov<sup>33</sup> for the general case of arbitrarily shaped particles. The analytical averaging of products of the amplitude scattering matrix elements over particle orientations is based on the use of the Clebsch–Gordan expansion<sup>25</sup>

$$d_{nm}^n(\beta) d_{m_1 m_1'}^{n'}(\beta) = \sum_{n_1=|n-n'|}^{n+n'} C_{nm m_1}^{n_1 m+m_1} C_{nm' m_1'}^{n_1 m'+m_1'} d_{m+m_1, m'+m_1'}^{n_1}(\beta) \quad (48)$$

and the orthogonality relation

$$\int_0^\pi d\beta \sin \beta d_{nm}^n(\beta) d_{m_1 m_1'}^{n'}(\beta) = \delta_{nn'} \frac{2}{2n+1}, \quad (49)$$

where  $C$ s are the well known Clebsch–Gordan coefficients which can be efficiently computed using recurrence formulas given in Ref. 25. In addition, Mishchenko<sup>24</sup> has explicitly used Eqs. (30) and (31) valid for rotationally symmetric particles to further considerably simplify the final equations. Furthermore, instead of directly computing the Stokes scattering matrix elements, Mishchenko<sup>24</sup> first computes the expansion coefficients appearing in the following expansions:<sup>34–36</sup>

$$a_1(\Theta) = \sum_{s=0}^{s_{\max}} \alpha_1^s P_{00}^s(\cos \Theta) = \sum_{s=0}^{s_{\max}} \alpha_1^s P_s(\cos \Theta), \quad (50)$$

$$a_2(\Theta) + a_3(\Theta) = \sum_{s=2}^{s_{\max}} (\alpha_2^s + \alpha_3^s) P_{22}^s(\cos \Theta), \quad (51)$$

$$a_2(\Theta) - a_3(\Theta) = \sum_{s=2}^{s_{\max}} (\alpha_2^s - \alpha_3^s) P_{2,-2}^s(\cos \Theta), \quad (52)$$

$$a_4(\Theta) = \sum_{s=0}^{s_{\max}} \alpha_4^s P_{00}^s(\cos \Theta), \quad (53)$$

$$b_1(\Theta) = \sum_{s=2}^{s_{\max}} \beta_1^s P_{02}^s(\cos \Theta), \quad (54)$$

$$b_2(\Theta) = \sum_{s=2}^{s_{\max}} \beta_2^s P_{02}^s(\cos \Theta), \quad (55)$$

where the upper summation limit  $s_{\max}$  depends on the desired accuracy of computations, and  $P_{pq}^s(x)$  are generalized spherical functions<sup>34,37</sup> expressed in terms of Wigner  $d$  functions as

$$P_{pq}^s(\cos \Theta) = i^{p-q} d_{pq}^s(\Theta). \quad (56)$$

[Note that Eq. (50) is the well known expansion of the phase function in Legendre polynomials  $P_s(\cos \Theta)$ .<sup>38-40</sup>] This approach has several important advantages. First, if the expansion coefficients in Eqs. (50)–(55) are known, then the scattering matrix can be easily computed for essentially any number of scattering angles with a minimal expense of CPU time. Second, the expansion coefficients are very useful in computing multiple scattering of (polarized) light in plane-parallel media since they allow one to efficiently and accurately calculate the Fourier components of the phase matrix appearing in the Fourier decomposition of the (vector) radiative transfer equations.<sup>35,41,42</sup> Third, both the expansion coefficients and the  ${}^1T$  matrix elements are independent of the states of polarization of the incident and scattered beams and of the scattering angle, and, therefore, one may expect a direct relationship between the expansion coefficients on one hand and the  ${}^1T$  matrix elements on the other. And indeed, Mishchenko<sup>24</sup> has derived simple analytical formulas directly expressing the expansion coefficients for randomly oriented particles in the elements of the  ${}^1T$  matrix computed in the natural reference frame. As a result, computation of the highly complicated angular structure of light scattered by a nonspherical particle in a fixed orientation (see Sec. 5) with further numerical integration over particle orientations is avoided, thus making the analytical averaging method very accurate and fast. The most time-consuming part in any computations based on the  $T$ -matrix method is evaluation of multiple nested summations, and a very important advantage of the Mishchenko formulation is that the maximal order of nested summations in the final equations is only three. This makes the analytical approach ideally suitable for developing an efficient computer code.<sup>24,43†</sup> Direct comparisons of the Mishchenko analytical method and the straightforward orientational averaging procedure using numerical angular integrations<sup>11</sup> have shown that the analytical method is faster by a factor of several tens.<sup>44</sup>

The analytical orientation averaging approach based on Eq. (26) and the Clebsch–Gordan expansion of Eq. (48) was also used by Fucile et al<sup>45</sup> to compute light scattering by an assembly of linear chains of small spheres.

The problem of computing the extinction matrix for nonspherical particles axially oriented by magnetic and gravitational/aerodynamical forces was studied in Refs. 46 and 47. An axially symmetric orientation distribution is given by a distribution function

$$P(\alpha, \beta, \gamma) = \frac{1}{4\pi^2} p(\beta), \quad (57)$$

which, along with Eqs. (26) and (48), leads to the following simple formula for the orientationally averaged  $T$  matrix:

$$\begin{aligned} \langle {}^2T_{mm'n'}^{ij} \rangle &= \int_0^{2\pi} d\alpha \int_0^\pi d\beta \sin \beta \int_0^{2\pi} d\gamma {}^2T_{mm'n'}^{ij}(\alpha, \beta, \gamma) P(\alpha, \beta, \gamma) \\ &= \delta_{mm'} \sum_{m_1=-M}^M \sum_{n_1=|n-n'|}^{n+n'} (-1)^{m+m_1} p_{n_1} C_{mm'n'-m_1}^{n_1 0} C_{nm_1 n'-m_1}^{n_1 0} {}^1T_{m_1 nm_1 n'}^{ij}, \end{aligned} \quad (58)$$

where  $M = \min(n, n')$  and

$$p_n = \int_0^\pi d\beta \sin \beta p(\beta) d_{00}^n(\beta) \quad (59)$$

†The computer code described in Ref. 43 is available from the first author upon request.

are coefficients in the expansion of the function  $p(\beta)$  in Legendre polynomials:

$$p(\beta) = \sum_{n=0}^{\infty} \frac{2n+1}{2} p_n P_n(\cos \beta). \quad (60)$$

Equations (22) and (58) along with the optical theorem are then used to express the extinction matrix elements in the elements of the forward-scattering amplitude matrix.<sup>46</sup> Again, the computer code based on the analytical orientation averaging method was found to be very accurate and fast. Equation (58) was later used by Fucile et al<sup>48</sup> to compute the forward-scattering amplitude matrix elements for small sphere aggregates exposed to an external electrostatic field.

Recently, the analytical approach developed in Refs. 24 and 33 for randomly oriented and in Ref. 46 for axially oriented nonspherical particles has been straightforwardly extended by Paramonov<sup>30</sup> to arbitrary quadratically integrable orientation distribution functions. However, Paramonov's equations involve highly nested summations, and their efficient numerical implementation may well be problematic. In this case, the standard averaging approach using numerical angular integrations can be more efficient. This approach<sup>11,49</sup> is based on the facts that averaging over particle orientations is equivalent to averaging over directions of light incidence and scattering and that the knowledge of the particle natural  $T$  matrix enables computations of the amplitude scattering matrix for any direction of light incidence and scattering with respect to the natural coordinate system [Eq. (22)].

Finally, it should be noted that Eqs. (7) and (8) are not the only possible representation of vector spherical functions. Other representations which differ by normalization and/or are linear combinations of each other and, therefore, result in somewhat different  $T$  matrices have been used (see, e.g., Refs. 50–54). We have used the vector spherical functions given by Eqs. (7) and (8) because their exponential azimuth-angle dependence makes them ideally suitable for analytical averaging over particle orientations.

### 3. COMPUTATION OF THE $T$ MATRIX FOR SINGLE SCATTERERS

The attractive mathematical formalism outlined in the preceding section would be essentially useless in the absence of efficient numerical techniques to compute the  $T$  matrix for nonspherical particles. Fortunately, several such techniques have been developed for both single and aggregated particles. In this section we will discuss the computation of the  $T$  matrix for single particles, while the following section will deal with aggregated/composite scatterers.

The standard scheme for computing the  $T$  matrix for single scatterers in the natural reference frame is based on the extended boundary condition method (EBCM) first developed by Waterman<sup>12–14</sup> for homogeneous particles (see also Refs. 51 and 55). In addition to the expansion of the incident and scattered fields given by Eqs. (5) and (6), the internal field is also expanded in vector spherical functions:

$$\mathbf{E}^{\text{int}}(\mathbf{R}) = \sum_{n=1}^{\infty} \sum_{m=-n}^n [c_{mn} \text{Rg } \mathbf{M}_{mn}(m, k\mathbf{R}) + d_{mn} \text{Rg } \mathbf{N}_{mn}(m, k\mathbf{R})], \quad (61)$$

where  $m_r$  is the refractive index of the particle relative to that of the surrounding medium. The relation between the expansion coefficients of the incident and internal fields is linear and, in compact matrix notation, is given by

$$\begin{bmatrix} \mathbf{a} \\ \mathbf{b} \end{bmatrix} = \begin{bmatrix} \mathbf{Q}^{11} & \mathbf{Q}^{12} \\ \mathbf{Q}^{21} & \mathbf{Q}^{22} \end{bmatrix} \begin{bmatrix} \mathbf{c} \\ \mathbf{d} \end{bmatrix}, \quad (62)$$

where the elements of the matrix  $\mathbf{Q}$  are two-dimensional integrals which must be numerically evaluated over the particle surface and depend on the particle size, shape, refractive index, and orientation with respect to the natural reference frame. Analogously, the scattered field coefficients are expressed in the internal field coefficients as

$$\begin{bmatrix} \mathbf{p} \\ \mathbf{q} \end{bmatrix} = - \begin{bmatrix} \text{Rg } \mathbf{Q}^{11} & \text{Rg } \mathbf{Q}^{12} \\ \text{Rg } \mathbf{Q}^{21} & \text{Rg } \mathbf{Q}^{22} \end{bmatrix} \begin{bmatrix} \mathbf{c} \\ \mathbf{d} \end{bmatrix}, \quad (63)$$



where, again, the elements of the  $\text{Rg } \mathbf{Q}$  matrix are two-dimensional integrals over the particle surface. Comparing Eqs. (62) and (63) with Eq. (20), we finally obtain

$$\mathbf{T} = -\text{Rg } \mathbf{Q}[\mathbf{Q}]^{-1}. \quad (64)$$

General formulas for computing the matrices  $\mathbf{Q}$  and  $\text{Rg } \mathbf{Q}$  for particles of any shape are given in Ref. 17. In the case of rotationally symmetric particles, the formulae become much simpler provided that the  $z$  axis of the natural coordinate system coincides with the axis of particle symmetry [cf. Eqs. (30) and (31)]. This simplicity explains why nearly all numerical results computed with the  $T$ -matrix approach pertain to bodies of revolution. It appears that Refs. 56 and 57 are the only papers which report the investigation of light scattering by particles without rotational symmetry (general ellipsoids). Peterson and Ström<sup>58</sup> (see also Refs. 59–61) generalized the EBCM to multilayered scatterers, while Lakhtakia et al<sup>62</sup> applied it to light scattering by chiral particles.

As pointed out in Refs. 63 and 64, in computations for nonspherical particles in a fixed orientation the  $T$ -matrix approach can be more than two orders of magnitude faster than the separation of variables method for spheroids<sup>22</sup> and several orders of magnitude faster than the discrete dipole approximation/volume integral equation formulation.<sup>19–21</sup> Moreover, we have directly compared the efficiency of computer codes based on the EBCM and the version of the separation of variables method for spheroids described in Ref. 23 by computing the same cases on the same computer (IBM RISC model 37T workstation). The comparison has shown that in computations for moderately aspherical spheroids in a fixed orientation the  $T$ -matrix approach can be faster by a factor exceeding 10. This superiority of the  $T$ -matrix approach over the separation of variables method and the discrete dipole approximation/volume integral equation formulation is further reinforced by the availability of the highly efficient analytical procedure for averaging light scattering characteristics over particle orientations, as described in the previous section. The superior numerical efficiency of the EBCM is accompanied by high numerical accuracy. Therefore, the EBCM has been used to tabulate results of benchmark computations for spheroidal and Chebyshev particles<sup>24,65,66</sup> which are suitable for testing computer codes based on other accurate or approximate methods.

The only disadvantage of the EBCM is its poor numerical stability in computations for particles that have very large real and/or imaginary parts of the refractive index, are large compared with a wavelength, and/or have extreme geometries such as prolate and oblate spheroids with large aspect ratios. The origin of this poor stability can be explained as follows. Although in principle the expansions of Eqs. (5), (6), and (61) are infinite, in practical computer calculations they must be truncated to a finite maximum size. This maximum size depends on the required accuracy of computations and is determined by increasing the size of the matrices  $\mathbf{Q}$  and  $\text{Rg } \mathbf{Q}$  in a unit step until some convergence criteria (such as those described in Refs. 11 and 43) are satisfied. Unfortunately, different elements of the matrix  $\mathbf{Q}$  can differ by many orders of magnitude, thus making the calculation of the inverse matrix  $\mathbf{Q}^{-1}$  an ill-conditioned process strongly influenced by round-off errors (e.g., Ref. 67). The ill-conditionality means that even small numerical errors in the computed elements of the matrix  $\mathbf{Q}$  may result in (very) large errors in the elements of the inverse matrix  $\mathbf{Q}^{-1}$ . The round-off errors become increasingly significant with increasing particle size parameter and/or aspect ratio and rapidly accumulate with increasing size of the matrix  $\mathbf{Q}$ . As a result, for large and/or highly aspherical particles, for which the required convergent size of the  $T$  matrix must be large,  $T$ -matrix computations can become slowly convergent or even divergent.<sup>5,11,68</sup>

One approach for overcoming the problem of numerical instability in computing the  $T$  matrix for highly elongated spheroids is the so-called iterative extended boundary condition method (IEBCM).<sup>69–74</sup> The main feature of this technique is a representation of the internal field by several subdomain spherical function expansions centered on the major axis of the prolate spheroid. These subregional expansions are linked to each other by being explicitly matched in the appropriate overlapping zones. The numerical details of the technique can be found in Ref. 69. The IEBCM has been used to compute light scattering and absorption by highly elongated lossy and low-loss dielectric scatterers with aspect ratios as large as 17. It has been shown that in some cases the use of IEBCM instead of the regular extended boundary condition method allows to more than

quadruple the maximum convergent size parameter. The disadvantage of this technique is that its numerical stability is achieved at the expense of a considerable increase in computer code complexity and required CPU time.

Another technique for dealing with the numerical instability of the regular extended boundary condition technique explicitly uses the unitarity property of the  $T$  matrix for nonabsorbing particles given by Eq. (45).<sup>75-77</sup> This technique involves iterative orthogonalization of the  $T$  matrix using the modified Gram-Schmidt reinforced orthogonalization method,<sup>76,77</sup> is simple and computationally efficient, and results in numerically stable  $T$  matrices for highly elongated and flattened spheroids. Convergent computations have been reported for aspect ratios as large as 20. The only disadvantage of this simple and powerful technique is that it can be applied only to perfectly conducting or lossless dielectric scatterers.

Recently, we have demonstrated that an efficient method for dealing with the ill-conditioning of the numerical inversion of the matrix  $Q$  is to improve the accuracy with which this matrix is calculated and inverted.<sup>78</sup> Specifically, we calculated the elements of this matrix and performed the matrix inversion using extended precision (REAL\*16 and COMPLEX\*32) instead of double-precision (REAL\*8 and COMPLEX\*16) floating-point variables. These calculations were performed on IBM RISC workstations for which the accuracy of double-precision and extended-precision variables is approximately 15 and 31 decimal digits, respectively. Extensive computations for prolate and oblate spheroids with different aspect ratios and refractive indices have shown that the use of extended precision instead of double precision variables more than doubles the maximum size parameter (i.e., the ratio of particle circumference to wavelength of scattered light for the surface- or volume-equivalent sphere) for which convergence of  $T$ -matrix computations can be achieved. Depending on refractive index and aspect ratio, this maximum size parameter can well exceed 50.

The effect of using extended precision variables is demonstrated in Fig. 1 which shows the relative accuracy of computing the extinction and scattering cross sections for randomly oriented prolate

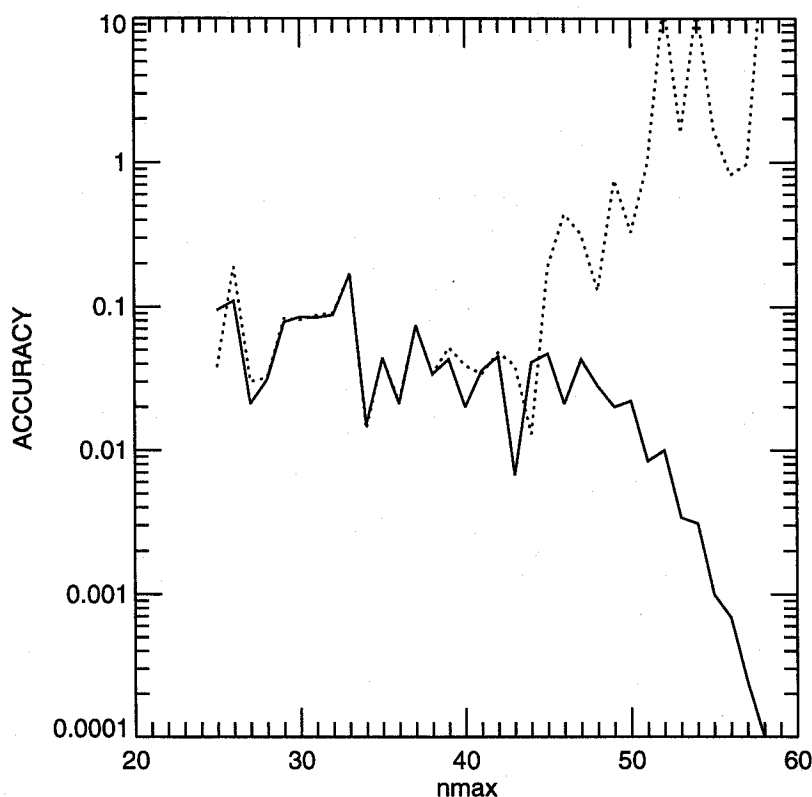


Fig. 1. Relative accuracy of computing the extinction and scattering cross sections for randomly oriented prolate spheroids with aspect ratio 4 and equal-surface-area-sphere size parameter 16 vs the largest  $n$ -value in Eqs. (5), (6), and (61). (—) and (·····) show results obtained using extended-precision and double-precision floating point variables, respectively.

spheroids with aspect ratio (ratio of the largest to the smallest spheroidal axes) 4 as a function of the maximum  $n$ -value in expansions (5), (6), and (61).<sup>78</sup> The refractive index of the spheroids is  $1.5 + 0.02i$  and their equal-surface-area-sphere size parameter is 16. One sees that, for these spheroids, double-precision computations cannot provide accuracy better than  $10^{-2}$  whereas the use of extended-precision arithmetic can give accuracy better than  $10^{-4}$ .

As discussed by Mishchenko and Travis,<sup>78</sup> the use of extended-precision instead of double-precision variables requires only a negligibly small extra memory. Timing tests performed on an IBM RISC Model 37T workstation show that the use of extended-precision arithmetic slows computations down by a factor of only 5–6, which is certainly a tolerable cost for being able to compute much larger nonspherical particles than ever before. Of course, a key feature of this approach is its simplicity and the fact that little additional programming effort is required.

The power of this approach is demonstrated in Figs. 2 and 3. Figure 2 shows the elements of the Stokes scattering matrix  $F$  [see Eq. (46)] computed for randomly oriented oblate spheroids with aspect ratio 2, equal-surface-area-sphere size parameter 80, and refractive index  $1.394 + 0.00685i$  corresponding to water ice at  $\lambda = 3.732 \mu\text{m}$ .<sup>79</sup> Figure 3 depicts analogous computations for randomly oriented finite cylinders with diameter-to-length ratio 1, equal-surface-area-sphere size parameter 75, and the same refractive index  $1.394 + 0.00685i$ . The computation of Figs. 2 and 3 with a scattering angle step size of  $0.1^\circ$  took 12 hours of CPU time on an IBM RISC model 37T workstation.  $T$ -matrix computations for particles this large can be used to investigate the range of applicability of the geometric optics approximation<sup>1,2</sup> in computing light scattering by nonspherical particles.<sup>80</sup> So far, direct comparisons of rigorous and ray tracing computations have been reported only for perfect spheres<sup>3</sup> and infinite circular cylinders.<sup>81</sup>

There is no doubt that light scattering by even bigger nonspherical particles can be calculated using computer variables with a larger number of decimal digits or by employing the IEBCM or

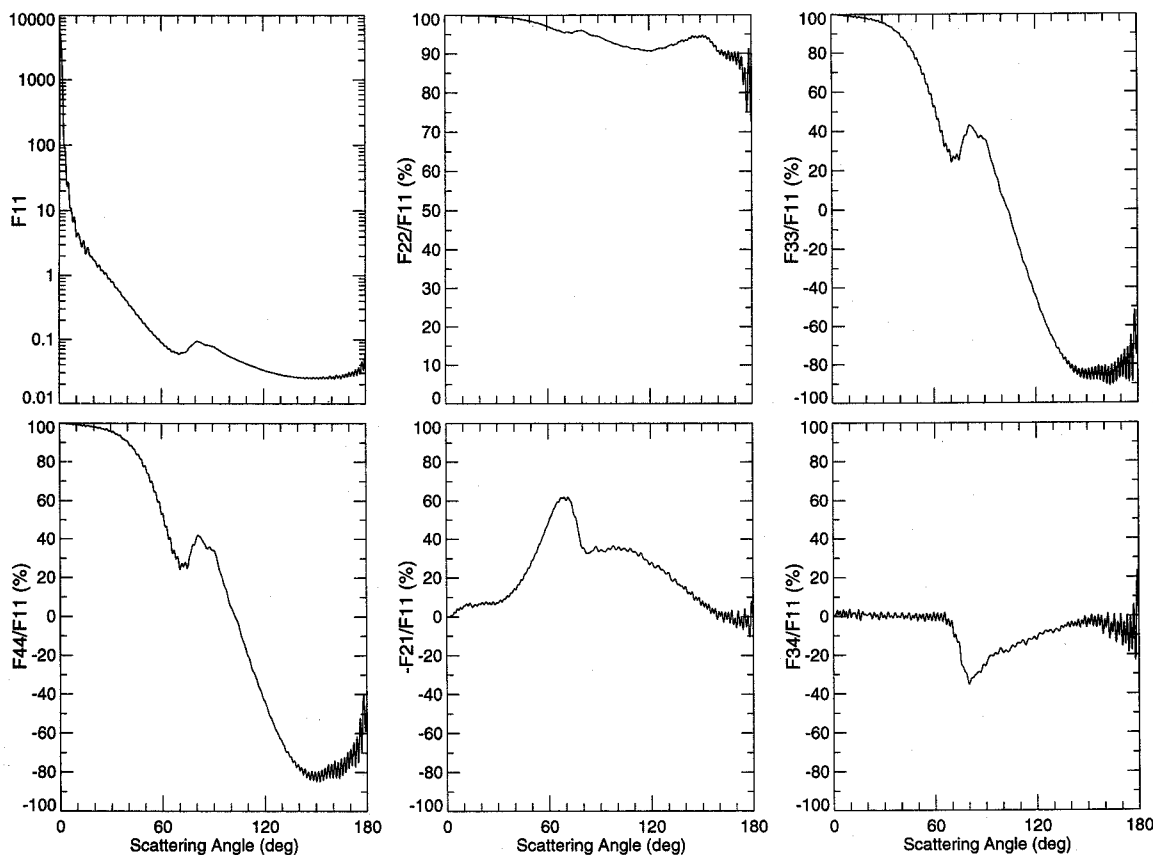


Fig. 2. Elements of the normalized scattering matrix given by Eq. (46) vs scattering angle for monodisperse, randomly oriented oblate spheroids with aspect ratio 2, equal-surface-area-sphere size parameter 80, and refractive index  $1.394 + 0.00685i$ .

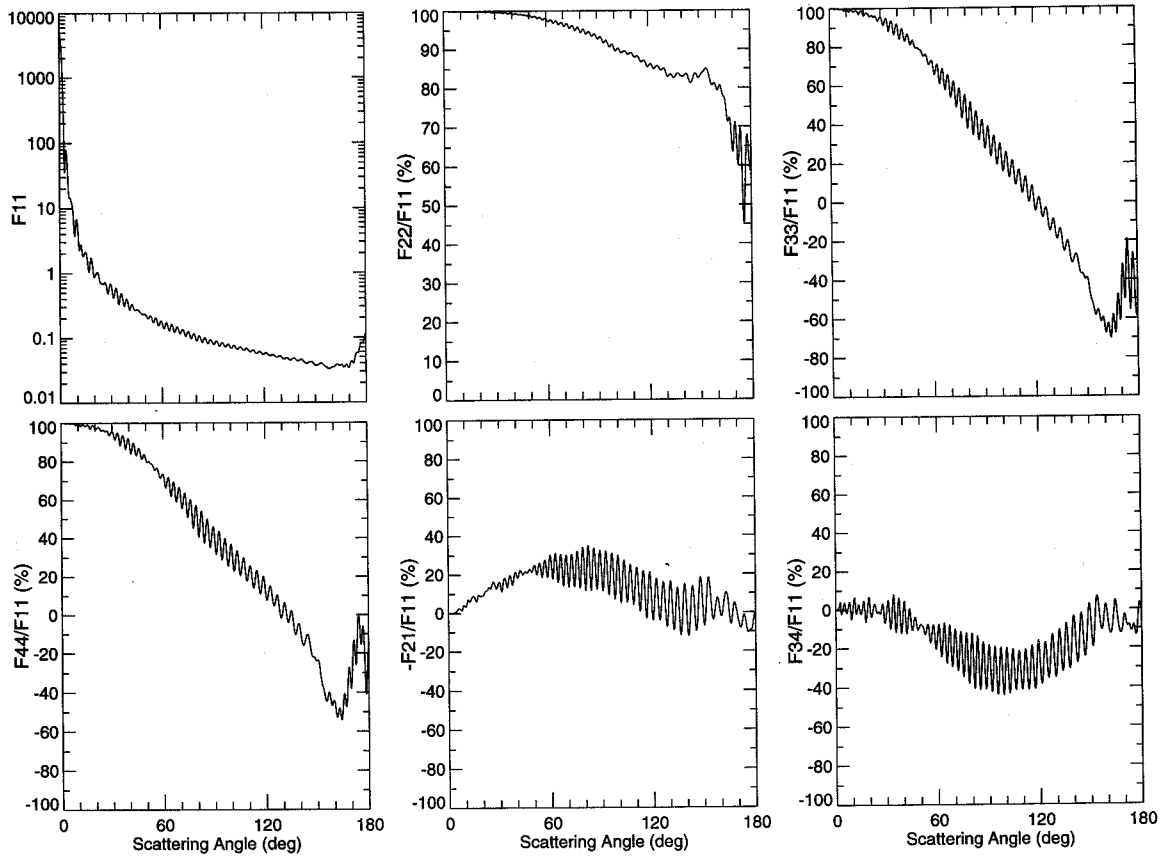


Fig. 3. As in Fig. 2, but for randomly oriented circular cylinders with equal-surface-area-sphere size parameter 75 and diameter-to-length ratio 1.

the method of iterative orthogonalization for nonabsorbing scatterers, but this would naturally be at the expense of a further increase of required CPU time.

#### 4. AGGREGATED/COMPOSITE PARTICLES

According to Eqs. (23) and (25), vector spherical functions in a rotated coordinate system can easily be expanded in vector spherical functions in the original coordinate system and this expansion can be used to derive the rotation transformation rule for the  $T$  matrix [Eq. (26)]. Similarly, vector spherical functions in a translated coordinate system can be expanded in vector spherical functions in the original coordinate system with the aid of the translation addition theorem and this can be used to derive a translation transformation rule for the  $T$  matrix and to develop a superposition  $T$ -matrix scheme to compute light scattering by composite/aggregated particles. Application of this approach was reported first in Refs. 82 and 83 for the case of a two-sphere cluster and in Ref. 84 (see also Ref. 85) for the general case of a cluster composed of an arbitrary number of nonspherical components. Note that in the case of a cluster with spherical components, the superposition  $T$ -matrix approach is equivalent to the separation of variables method.

The basic idea of this approach is as follows.<sup>84</sup> Consider a cluster of  $N$  arbitrarily shaped scattering particles illuminated by a plane external electromagnetic wave, and suppose that the  $T$  matrices of each of the component particles are known in their respective local coordinate systems with origins inside the particles. We also assume that all the local coordinate systems have the same spatial orientation and that the smallest circumscribing spheres of the component particles centered at the origins of their local coordinate systems do not overlap. The total field scattered by the whole cluster can be given as a superposition of individual fields scattered from each particle:

$$\mathbf{E}^{\text{sca}} = \sum_{j=1}^N \mathbf{E}_j^{\text{sca}}. \quad (65)$$

Because of electromagnetic interactions between the particles, the individual scattered fields are interdependent and the electric field exciting each particle is the superposition of the external field  $\mathbf{E}_0^{\text{inc}}$  and the sum of the individual fields scattered by all other particles:

$$\mathbf{E}_j^{\text{inc}} = \mathbf{E}_0^{\text{inc}} + \sum_{l \neq j} \mathbf{E}_l^{\text{sca}}, \quad j = 1, \dots, N. \quad (66)$$

To exploit the information content of the  $j$ th particle  $T$  matrix, we must expand the fields incident on and scattered by this particle in vector spherical functions centered at the origin of the particle local coordinate system:

$$\begin{aligned} \mathbf{E}_j^{\text{inc}} &= \sum_{nm} [a_{mn}^j \text{Rg } \mathbf{M}_{mn}(k\mathbf{R}_j) + b_{mn}^j \text{Rg } \mathbf{N}_{mn}(k\mathbf{R}_j)] \\ &= \sum_{nm} \left[ \left( a_{mn}^{j0} + \sum_{l \neq j} a_{mn}^{jl} \right) \text{Rg } \mathbf{M}_{mn}(k\mathbf{R}_j) \right. \\ &\quad \left. + \left( b_{mn}^{j0} + \sum_{l \neq j} b_{mn}^{jl} \right) \text{Rg } \mathbf{N}_{mn}(k\mathbf{R}_j) \right], \quad j = 1, \dots, N, \end{aligned} \quad (67)$$

$$\mathbf{E}_j^{\text{sca}} = \sum_{nm} [p_{mn}^j \mathbf{M}_{mn}(k\mathbf{R}_j) + q_{mn}^j \mathbf{N}_{mn}(k\mathbf{R}_j)], \quad R_j > r_j, \quad j = 1, \dots, N, \quad (68)$$

where the radius vector  $\mathbf{R}_j$  originates at the origin of the  $j$ th particle local coordinate system,  $r_j$  is the radius of the smallest circumscribing sphere of the  $j$ th particle, the expansion coefficients  $a_{mn}^{j0}$  and  $b_{mn}^{j0}$  describe the external incident field, and the expansion coefficients  $a_{mn}^{jl}$  and  $b_{mn}^{jl}$  describe the contribution of the  $l$ th particle to the field illuminating the  $j$ th particle:

$$\mathbf{E}_0^{\text{inc}} = \sum_{nm} [a_{mn}^{j0} \text{Rg } \mathbf{M}_{mn}(k\mathbf{R}_j) + b_{mn}^{j0} \text{Rg } \mathbf{N}_{mn}(k\mathbf{R}_j)], \quad j = 1, \dots, N, \quad (69)$$

$$\mathbf{E}_l^{\text{sca}} = \sum_{nm} [a_{mn}^{jl} \text{Rg } \mathbf{M}_{mn}(k\mathbf{R}_j) + b_{mn}^{jl} \text{Rg } \mathbf{N}_{mn}(k\mathbf{R}_j)], \quad j, l = 1, \dots, N. \quad (70)$$

The relation between the expansion coefficients of the illuminating and scattered fields is given by the  $j$ th particle  $T$  matrix  $\mathbf{T}^j$ :

$$\begin{bmatrix} \mathbf{p}^j \\ \mathbf{q}^j \end{bmatrix} = \mathbf{T}^j \left\{ \begin{bmatrix} \mathbf{a}^{j0} \\ \mathbf{b}^{j0} \end{bmatrix} + \sum_{l \neq j} \begin{bmatrix} \mathbf{a}^{jl} \\ \mathbf{b}^{jl} \end{bmatrix} \right\}, \quad j = 1, \dots, N. \quad (71)$$

The field scattered by the  $l$ th particle can also be expanded in vector spherical functions centered at the origin of the  $l$ th local coordinate system:

$$\mathbf{E}_l^{\text{sca}} = \sum_{\nu\mu} [p_{\mu\nu}^l \mathbf{M}_{\mu\nu}(k\mathbf{R}_l) + q_{\mu\nu}^l \mathbf{N}_{\mu\nu}(k\mathbf{R}_l)], \quad R_l > r_l, \quad (72)$$

where  $\mathbf{R}_l$  is the radius vector originating at the origin of the  $l$ th particle coordinate system. Using the translation addition theorem,<sup>86</sup> the vector spherical functions in Eq. (72) can be expanded in regular vector spherical functions originating inside the  $j$ th particle:

$$\mathbf{M}_{\mu\nu}(k\mathbf{R}_l) = \sum_{nm} [A_{mn\mu\nu}(k\mathbf{R}_{lj}) \text{Rg } \mathbf{M}_{mn}(k\mathbf{R}_j) + B_{mn\mu\nu}(k\mathbf{R}_{lj}) \text{Rg } \mathbf{N}_{mn}(k\mathbf{R}_j)], \quad R_j < R_{lj}, \quad (73)$$

$$\mathbf{N}_{\mu\nu}(k\mathbf{R}_l) = \sum_{nm} [B_{mn\mu\nu}(k\mathbf{R}_{lj}) \text{Rg } \mathbf{M}_{mn}(k\mathbf{R}_j) + A_{mn\mu\nu}(k\mathbf{R}_{lj}) \text{Rg } \mathbf{N}_{mn}(k\mathbf{R}_j)], \quad R_j < R_{lj}, \quad (74)$$

where the vector  $\mathbf{R}_{lj} = \mathbf{R}_l - \mathbf{R}_j$  connects the origins of the local coordinate systems of the  $l$ th and the  $j$ th particles, and the translation coefficients  $A_{mn\mu\nu}(k\mathbf{R}_{lj})$  and  $B_{mn\mu\nu}(k\mathbf{R}_{lj})$  can be computed using analytical expressions given on p. 449 of Ref. 17. Comparing Eqs. (70)–(74), we finally derive

$$\begin{bmatrix} \mathbf{p}^j \\ \mathbf{q}^j \end{bmatrix} = \mathbf{T}^j \left\{ \begin{bmatrix} \mathbf{a}^{j0} \\ \mathbf{b}^{j0} \end{bmatrix} + \sum_{l \neq j} \begin{bmatrix} \mathbf{A}(k\mathbf{R}_{lj}) & \mathbf{B}(k\mathbf{R}_{lj}) \\ \mathbf{B}(k\mathbf{R}_{lj}) & \mathbf{A}(k\mathbf{R}_{lj}) \end{bmatrix} \begin{bmatrix} \mathbf{p}^l \\ \mathbf{q}^l \end{bmatrix} \right\}, \quad j = 1, \dots, N. \quad (75)$$

Since the expansion coefficients of the external plane electromagnetic wave  $a_{mn}^{j0}$  and  $b_{mn}^{j0}$  and the translation coefficients  $A_{mn\mu\nu}(k\mathbf{R}_{lj})$  and  $B_{mn\mu\nu}(k\mathbf{R}_{lj})$  can be easily computed, Eq. (75) is a system of linear algebraic equations which can be solved for numerically to compute the expansion coefficients of the individual scattered fields  $p_{mn}^j$  and  $q_{mn}^j$  for each of the cluster components. When these coefficients are known, Eqs. (68) and (65) give the total field scattered by the cluster.

Equation (75) becomes especially simple for a cluster composed of spherical particles since in this case the individual  $T$  matrices are diagonal with standard Mie coefficients standing along the main diagonal [Eqs. (32)–(34)]. Solutions of Eq. (75) for clusters of spheres have been obtained using different numerical techniques (direct matrix inversion, method of successive orders of scattering, conjugate gradients method, method of iterations, recursive method) and have been extensively reported in the literature.<sup>87–106</sup> The number of spheres in a cluster was as large as several thousand. A detailed discussion of numerical aspects can be found in Refs. 87 and 91 while Ref. 90 contains a review of the history of dependent scattering by clusters of particles. Recently, Borghese et al<sup>107,108</sup> and Fuller<sup>109</sup> have extended the superposition approach to the case of internal aggregation by solving the problem of light scattering by spherical particles with eccentric spherical inclusions, while Videen et al<sup>110</sup> considered a more general case of a sphere with an irregular inclusion.<sup>†</sup>

Inversion of Eq. (75) gives<sup>96</sup>

$$\begin{bmatrix} \mathbf{p}^j \\ \mathbf{q}^j \end{bmatrix} = \sum_{l=1}^N \mathbf{T}^{jl} \begin{bmatrix} \mathbf{a}^{l0} \\ \mathbf{b}^{l0} \end{bmatrix}, \quad j = 1, \dots, N, \quad (76)$$

where the matrices  $\mathbf{T}^{jl}$  transform the expansion coefficients of the incident field centered at the  $l$ th particle into the  $j$ th-particle-centered expansion coefficients of the field scattered by the  $j$ th particle. Calculation of the matrices  $\mathbf{T}^{jl}$  requires numerical inversion of a large matrix and can be a time-consuming process. However, these matrices are independent of the incident field and depend only on the cluster configuration and shapes and orientations of the component particles. Therefore, the matrices  $\mathbf{T}^{jl}$  need be computed only once and then can be used in computations for any direction and polarization state of the incident field. They can also be used to analytically average the extinction and scattering cross sections over cluster orientations.<sup>96</sup>

Furthermore, in the far field region the scattered-field expansions from the individual particles can be transformed into a single expansion based on a single origin of the cluster. This single origin can represent the average of the component particle positions but in general can be arbitrary. The first step is to expand the incident and total scattered fields in vector spherical functions centered at the cluster origin:

$$\mathbf{E}_0^{\text{inc}} = \sum_{nm} [a_{nm} \text{Rg } \mathbf{M}_{nm}(k\mathbf{R}_0) + b_{nm} \text{Rg } \mathbf{N}_{nm}(k\mathbf{R}_0)], \quad (77)$$

$$\mathbf{E}^{\text{sca}} = \sum_{nm} [p_{nm} \mathbf{M}_{nm}(k\mathbf{R}_0) + q_{nm} \mathbf{N}_{nm}(k\mathbf{R}_0)], \quad (78)$$

where the radius vector  $\mathbf{R}_0$  originates at the origin of the cluster. We again employ the translation addition theorem given by

$$\text{Rg } \mathbf{M}_{mn}(k\mathbf{R}_0) = \sum_{\nu\mu} [\text{Rg } A_{\mu\nu mn}(k\mathbf{R}_{0l}) \text{Rg } \mathbf{M}_{\mu\nu}(k\mathbf{R}_l) + \text{Rg } B_{\mu\nu mn}(k\mathbf{R}_{0l}) \text{Rg } \mathbf{N}_{\mu\nu}(k\mathbf{R}_l)], \quad (79)$$

$$\text{Rg } \mathbf{N}_{mn}(k\mathbf{R}_0) = \sum_{\nu\mu} [\text{Rg } B_{\mu\nu mn}(k\mathbf{R}_{0l}) \text{Rg } \mathbf{M}_{\mu\nu}(k\mathbf{R}_l) + \text{Rg } A_{\mu\nu mn}(k\mathbf{R}_{0l}) \text{Rg } \mathbf{N}_{\mu\nu}(k\mathbf{R}_l)] \quad (80)$$

and by supplementary formulas

$$\mathbf{M}_{mn}(k\mathbf{R}_l) = \sum_{\nu\mu} [\text{Rg } A_{\mu\nu mn}(k\mathbf{R}_{j0}) \mathbf{M}_{\mu\nu}(k\mathbf{R}_0) + \text{Rg } B_{\mu\nu mn}(k\mathbf{R}_{j0}) \mathbf{N}_{\mu\nu}(k\mathbf{R}_0)], \quad R_0 > R_{j0}, \quad (81)$$

<sup>†</sup>Note that a sphere with a single eccentric inclusion can be considered a two-layered nonspherical particle and treated using the standard  $T$ -matrix approach for multilayered scatterers developed in Ref. 58.

$$N_{mn}(k\mathbf{R}_j) = \sum_{\nu\mu} [\text{Rg } B_{\mu\nu mn}(k\mathbf{R}_{j0}) \mathbf{M}_{\mu\nu}(k\mathbf{R}_0) + \text{Rg } A_{\mu\nu mn}(k\mathbf{R}_{j0}) \mathbf{N}_{\mu\nu}(k\mathbf{R}_0)], \quad R_0 > R_{j0}, \quad (82)$$

where  $\mathbf{R}_{0l} = \mathbf{R}_0 - \mathbf{R}_l$ ,  $\mathbf{R}_{j0} = \mathbf{R}_j - \mathbf{R}_0$ , and the translation coefficients  $\text{Rg } A_{\mu\nu mn}(k\mathbf{R}_{0l})$  and  $\text{Rg } B_{\mu\nu mn}(k\mathbf{R}_{0l})$  differ from  $A_{\mu\nu mn}(k\mathbf{R}_{0l})$  and  $B_{\mu\nu mn}(k\mathbf{R}_{0l})$  in that they are based on spherical Bessel functions rather than on spherical Hankel functions. We then easily derive

$$\begin{bmatrix} \mathbf{a}^0 \\ \mathbf{b}^0 \end{bmatrix} = \begin{bmatrix} \text{Rg } \mathbf{A}(k\mathbf{R}_{0l}) & \text{Rg } \mathbf{B}(k\mathbf{R}_{0l}) \\ \text{Rg } \mathbf{B}(k\mathbf{R}_{0l}) & \text{Rg } \mathbf{A}(k\mathbf{R}_{0l}) \end{bmatrix} \begin{bmatrix} \mathbf{a} \\ \mathbf{b} \end{bmatrix}, \quad l = 1, \dots, N, \quad (83)$$

$$\begin{bmatrix} \mathbf{p} \\ \mathbf{q} \end{bmatrix} = \sum_{j=1}^N \begin{bmatrix} \text{Rg } \mathbf{A}(k\mathbf{R}_{j0}) & \text{Rg } \mathbf{B}(k\mathbf{R}_{j0}) \\ \text{Rg } \mathbf{B}(k\mathbf{R}_{j0}) & \text{Rg } \mathbf{A}(k\mathbf{R}_{j0}) \end{bmatrix} \begin{bmatrix} \mathbf{p}^j \\ \mathbf{q}^j \end{bmatrix}. \quad (84)$$

Finally, using Eqn. (76)–(78), (83), and (84) we obtain<sup>84,96</sup>

$$\begin{bmatrix} \mathbf{p} \\ \mathbf{q} \end{bmatrix} = \mathbf{T} \begin{bmatrix} \mathbf{a} \\ \mathbf{b} \end{bmatrix}, \quad (85)$$

where the cluster *T* matrix is given by

$$\mathbf{T} = \sum_{j,l=1}^N \begin{bmatrix} \text{Rg } \mathbf{A}(k\mathbf{R}_{j0}) & \text{Rg } \mathbf{B}(k\mathbf{R}_{j0}) \\ \text{Rg } \mathbf{B}(k\mathbf{R}_{j0}) & \text{Rg } \mathbf{A}(k\mathbf{R}_{j0}) \end{bmatrix} \mathbf{T}^{jl} \begin{bmatrix} \text{Rg } \mathbf{A}(k\mathbf{R}_{0l}) \text{Rg } \mathbf{B}(k\mathbf{R}_{0l}) \\ \text{Rg } \mathbf{B}(k\mathbf{R}_{0l}) \text{Rg } \mathbf{A}(k\mathbf{R}_{0l}) \end{bmatrix}. \quad (86)$$

The main advantage of this cluster *T* matrix is that it can be used in Eq. (22) to compute the amplitude scattering matrix and in the analytical procedure for computing the orientationally averaged light scattering characteristics described in Sec. 2.<sup>96,111</sup> This advantage was fully realized by Mishchenko et al.,<sup>112</sup> who report and discuss extensive computations of light scattering by randomly oriented bispheres (two-sphere clusters) with touching and separated components.

Plate 1 demonstrates the performance of the analytical averaging procedure described in Ref. 111 and shows the scattering matrix elements for randomly oriented monodisperse bispheres with distance *d* between the centers of the component spheres equal to 2, 2.5, 4, and 8 times their radius. The size parameter of the component spheres is 5 and their refractive index is  $1.5 + 0.005i$ . For comparison, black lines show Mie computations for a single sphere with the same refractive index and size parameter 5. It is seen that the influence of cooperative scattering is strongest for bispheres with touching components ( $d = 2r$ ) and rapidly diminishes with increasing *d* so that the component spheres become essentially independent scatterers at as small distance between their centers as four times their radius. The effect of increasing *d* is especially well demonstrated by computations for the ratio  $F_{22}/F_{11}$  which must be equal to 100% for single spheres but can be substantially smaller for nonspherical/aggregated particles. Also of interest is that the single-sphere scattering structure is clearly evident even for bispheres with touching components and is the dominant feature in all scattering matrix elements but the (2, 2)-element.<sup>112</sup>

Equations (5), (6), (20), and (79)–(82) can also be used to derive the translation transformation law for the *T* matrix analogous to the rotation transformation law given by Eq. (26). Suppose that the *T* matrix of an arbitrary (single or clustered) nonspherical particle is known in the coordinate system 1 and we seek the *T* matrix in a translated coordinate system 2 having the same spatial orientation as the system 1. After straightforward manipulations, we obtain

$${}^2\mathbf{T} = \begin{bmatrix} \text{Rg } \mathbf{A}(-k\mathbf{R}_{21}) & \text{Rg } \mathbf{B}(-k\mathbf{R}_{21}) \\ \text{Rg } \mathbf{B}(-k\mathbf{R}_{21}) & \text{Rg } \mathbf{A}(-k\mathbf{R}_{21}) \end{bmatrix} {}^1\mathbf{T} \begin{bmatrix} \text{Rg } \mathbf{A}(k\mathbf{R}_{21}) & \text{Rg } \mathbf{B}(k\mathbf{R}_{21}) \\ \text{Rg } \mathbf{B}(k\mathbf{R}_{21}) & \text{Rg } \mathbf{A}(k\mathbf{R}_{21}) \end{bmatrix}, \quad (87)$$

where the vector  $\mathbf{R}_{21}$  connects the origins of the coordinate system 2 and 1, respectively. Since the extinction and scattering cross sections averaged over all particle orientations must be independent of the choice of the coordinate system, Eqs. (42) and (43) can be used to derive the following two invariants with respect to translations of the coordinate system:

$$\sum_{nmj} {}^2T_{mmn}^{jj} = \sum_{nmj} {}^1T_{mmn}^{jj}, \quad (88)$$

$$\sum_{nmn'm'tj} |{}^2T_{mm'n'}^{ij}|^2 = \sum_{nmn'm'tj} |{}^1T_{mm'n'}^{ij}|^2. \quad (89)$$

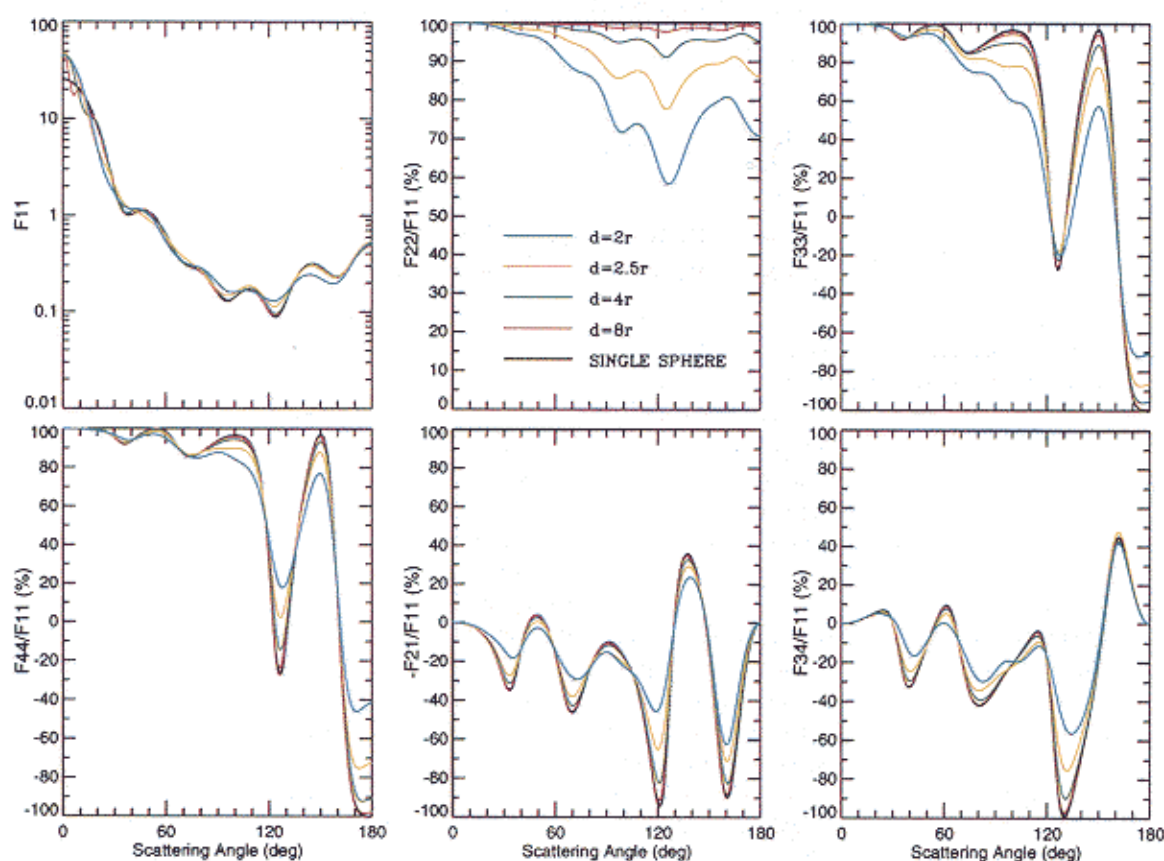


Plate 1. Elements of the scattering matrix for randomly oriented monodisperse bispheres with distance  $d$  between the centers of the component spheres equal to 2, 2.5, 4, and 8 times their radius. The size parameter of the component spheres is 5 and their refractive index is  $1.5 + 0.005i$ . Black lines show Mie computations for a single sphere with the same refractive index and size parameter 5. Note that for spheres  $F_{22}/F_{11} = 100\%$ .



An important modification of the *T*-matrix superposition method was developed in Refs. 113–115. Several alternative expressions for the transition matrix of a composite object were derived, which enabled the authors to avoid the geometrical constraints inherent in the standard approach. As a result, this technique can be applied to composite particles with concavo-convex components and can also be used in computations for particles with extreme geometries, e.g., highly elongated or flattened spheroids. In this regard, the technique can be considered a supplement to the methods for suppressing the numerical instability of the regular *T*-matrix approach described in the previous section.

## 5. NUMERICAL RESULTS

The high efficiency of the *T*-matrix approach has been employed by many authors to calculate light scattering by nonspherical particles with various shapes and sizes. Specifically, extensive computations for homogeneous and layered spheroids have been published in Refs. 5, 31, 46, 47, 59–61, 63, 66, 68–74, 76–78, and 116–136, while 43, 64, and 137–139 present a systematic study of spheroidal scattering based on numerical data for hundreds of thousands of randomly oriented spheroids with different aspect ratios and refractive indices. Illustrative scattering computations for finite circular cylinders were reported by Geller et al.<sup>121</sup> and Rupp,<sup>140</sup> while Kuik et al.<sup>141</sup> calculated and analysed light scattering by several tens of finite cylinders in random orientation with aspect ratios varying from 1 to 7. The shape of spheroids and finite cylinders is fully described by only one parameter (the ratio of the largest to the smallest axes  $\epsilon$  for spheroids and the diameter-to-length ratio for cylinders). By varying this single parameter, one can specify a wide variety of nonspherical shapes ranging from needles to plates, which makes spheroids and finite cylinders a convenient choice in modeling light scattering by convex bodies with major deviations of the shape from that of a sphere.

Wiscombe and Mugnai<sup>11,142–145</sup> computed and discussed scattering properties of several hundred rotationally symmetric particles obtained by continuously deforming a sphere by means of a Chebyshev polynomial of degree  $n$ . The shape of these so-called Chebyshev particles in the natural coordinate system is given by

$$r(\vartheta, \varphi) = r_0[1 + \xi T_n(\cos \vartheta)], \quad |\xi| < 1, \quad (90)$$

where  $r_0$  is the radius of the unperturbed sphere,  $\xi$  is the deformation parameter, and  $T_n(\cos \vartheta) = \cos n\vartheta$  is the Chebyshev polynomial of degree  $n$ . Two-dimensional drawings of different Chebyshev particles can be found in Refs. 11 and 143. All Chebyshev particles with  $n \geq 2$  become partially concave as the absolute value of the deformation parameter increases and exhibit surface roughness in the form of waves running completely around the particle. The number of waves increases linearly with increasing parameter  $n$  which, therefore, can be called the waviness parameter. Unfortunately, *T*-matrix computations for Chebyshev particles with  $|\xi|$  larger than 0.15–0.2 are poorly convergent and, thus, very slow. As a result, Chebyshev particles are best suited for examining the effect of microscopic roughness and mild concavity of the surface of nearly spherically shaped scatterers. Light scattering computations for monodisperse and polydisperse Chebyshev particles were also reported in Refs. 31, 64, 131, and 146.

Light scattering by aggregates composed of spherical particles was computed in Refs. 45, 48, and 87–109. Most of these references deal with aggregates in a fixed orientation, whereas some illustrative computations of orientationally averaged optical cross sections and amplitude and Stokes scattering matrix elements were reported in Refs. 45, 48, 101, and 109. The only detailed study of dependent scattering based on computations for hundreds of randomly oriented two-sphere clusters was published by Mishchenko et al.<sup>112</sup> who used the efficient analytical procedure for computing orientation-averaged cross sections and scattering matrix elements described in Refs. 96 and 111. Importantly, in addition to being composite particles, bispheres with touching components extensively studied in Ref. 112 can also be considered nonspherical particles with a strongly concave shape. Therefore, they constitute another class of nonspherical particles that distinctly differ from spheroids, finite cylinders, and Chebyshev particles and can be efficiently treated using the *T*-matrix method.

As was noted above, the *T*-matrix approach has been applied to compute benchmark results that can be used as accuracy checks in testing other rigorous or approximate methods for calculating

nonspherical scattering. Specifically, benchmark computations have been reported for randomly oriented monodisperse and polydisperse spheroids,<sup>24,65,66</sup> randomly oriented monodisperse Chebyshev particles,<sup>24,65</sup> and randomly oriented monodisperse bispheres with touching and separated components.<sup>147</sup>

The purpose of the rest of this section is to summarize and generalize the results of the extensive study of polydisperse spheroidal scattering published in Ref. 137 and to illustrate them by new computations for much larger particles performed with the recently improved *T*-matrix code.<sup>78</sup> All computations reported below pertain to a fixed refractive index of  $1.53 + 0.008i$  characteristic of dust-like tropospheric aerosols at visible wavelengths.<sup>148</sup> We begin with discussing the practical importance of computing light scattering by particles distributed over both sizes and orientations rather than by monodisperse particles in a fixed orientation, as emphasized in Refs. 3, 64, 144, 149, and 150. The most obvious reason for performing polydisperse rather than monodisperse computations is better modeling of natural particle ensembles in which particles are most often distributed over a range of sizes and orientations. The second reason comes from the fact that monodisperse scattering patterns are usually burdened with what is called the interference structure.<sup>1-3</sup> This effect is demonstrated in Plate 2(a), which shows the degree of linear polarization for single scattering of unpolarized incident light (i.e., the ratio  $-F_{21}/F_{11}$  of the elements of the scattering matrix) vs size parameter and scattering angle for monodisperse spheres with refractive index  $1.53 + 0.008i$ .<sup>†</sup> Plate 2(a) shows a field of sharp local minima and maxima which result from interference of light diffracted and reflected/transmitted by a particle,<sup>3</sup> thus making comparison of scattering characteristics for different monodisperse spheres problematic. For nonspherical particles the interference structure becomes even more complicated because now it depends not only on size parameter and scattering angle, but also on orientation of the particle with respect to incident and scattered beams. This is demonstrated in Plates 2(b) and 2(c) which show the degree of linear polarization vs scattering angle and equal-surface-area-sphere size parameter for monodisperse oblate spheroids with aspect ratio  $\epsilon = 1.7$  and two orientations of the spheroidal axis with respect to the incident beam. One indeed sees that the polarization patterns for the two spheroid orientations are totally different. Figure 4 shows the horizontal cross sections of Plates 2(a) and 2(b) corresponding to size parameter 30. It is seen that the polarization curves form a tangle of lines with no clear message and can hardly be used to derive useful conclusions about the effect of nonsphericity on light scattering.

Plate 2(d) shows that the polarization pattern computed for monodisperse oblate spheroids with  $\epsilon = 1.7$  in random orientation is smoother and less complicated than that for spheroids in a fixed orientation [Plates 2(b) and 2(c)]. As demonstrated in Plate 3 (diagram for oblate spheroids with  $\epsilon = 1.7$ ), this smoothing effect of averaging over orientations is obviously reinforced by the effect of averaging over sizes which totally removes the residual interference structure still seen in Plate 2(d). The result of size averaging for spheres is shown in Plate 4 (upper right panel). Contrasting Plates 2, 3, and 4, we can conclude that averaging over sizes for spherical particles and averaging over orientations and sizes for nonspherical particles smoothes the interference structure out and enables meaningful comparisons of scattering properties of different particles.

Note that in averaging over particle sizes we used a modified power law size distribution given by

$$n(x) = \begin{cases} C & \text{for } x \leq x_1, \\ C(x/x_1)^{-3} & \text{for } x_1 \leq x \leq x_2, \\ 0 & \text{for } x \geq x_2, \end{cases} \quad (91)$$

where  $x$  is size parameter for spherical particles and equal-surface-area-sphere size parameter for spheroids,  $n(x) dx$  is the fraction of the particles with size parameters between  $x$  and  $x + dx$ , and  $C$  is a normalization constant such that

$$\int_0^\infty dx n(x) = 1. \quad (92)$$

<sup>†</sup>Note that the use of discrete colors in Plates 2–9 enables convenient and easy quantification of the color diagrams using the white color as the reference.

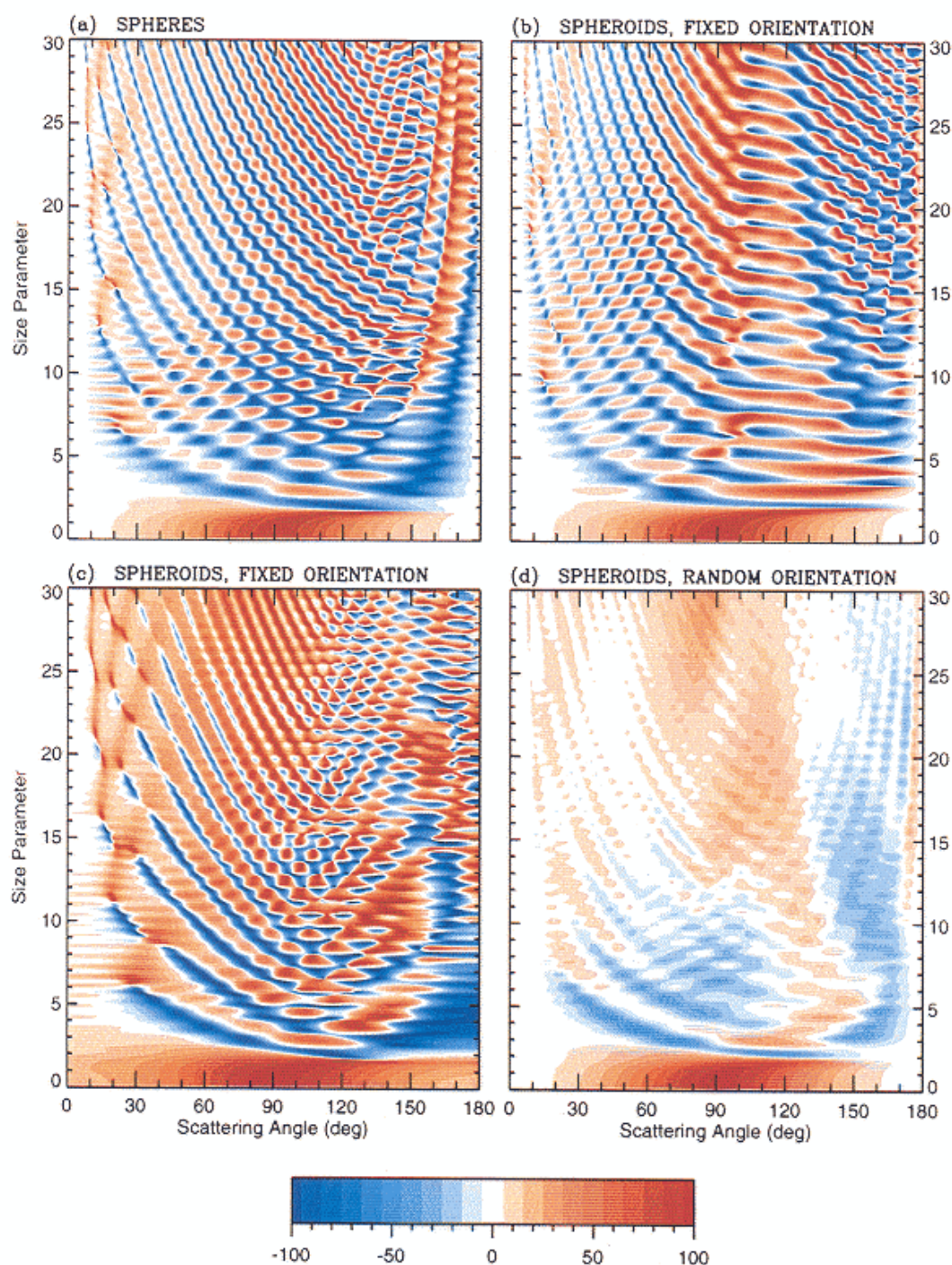


Plate 2. Degree of linear polarization vs scattering angle and size parameter for monodisperse spheres and surface-equivalent oblate spheroids in fixed and random orientations. In panel (b) the spheroid axis is parallel to the incident beam and the scattering plane is an arbitrary plane through this beam, while in panel (c) the spheroid axis is perpendicular to the direction of light incidence and the scattering plane is defined as the plane through the axis and the incident beam. The refractive index is  $1.53 + 0.008i$  and the spheroid aspect ratio is 1.7.

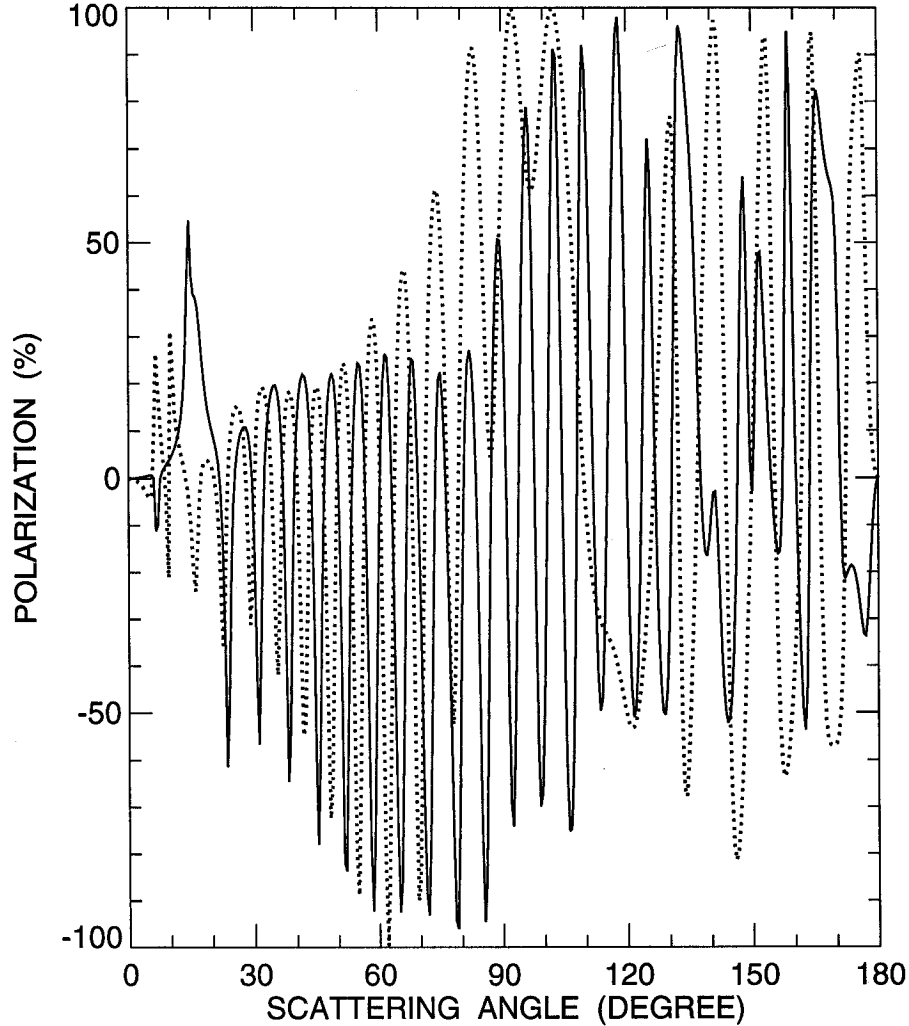


Fig. 4. Degree of linear polarization vs scattering angle for a monodisperse sphere (—) and an equal-surface-area oblate spheroid with aspect ratio 1.7 (····). The sphere size parameter is 30 and the index of refraction for both particles is  $1.53 + 0.008i$ . The spheroid axis is parallel to the direction of the incident light and the scattering plane is an arbitrary plane through this beam.

Hansen and Travis<sup>3</sup> and Mishchenko and Travis<sup>137</sup> have shown that in practice, most plausible size distributions of spheres and spheroids can be adequately represented by just two parameters, the effective size parameter  $x_{\text{eff}}$  and effective variance  $v_{\text{eff}}$ , defined as<sup>3</sup>

$$x_{\text{eff}} = \frac{1}{G} \int_0^{\infty} dx \pi x^3 n(x), \quad (93)$$

$$v_{\text{eff}} = \frac{1}{G x_{\text{eff}}^2} \int_0^{\infty} dx (x - x_{\text{eff}})^2 \pi x^2 n(x), \quad (94)$$

where

$$G = \int_0^{\infty} dx \pi x^2 n(x). \quad (95)$$

In other words, different size distributions that have the same values of the effective size parameter and effective variance have essentially identical scattering properties. Therefore, instead of characterizing the size distribution given by Eq. (91) by the formal parameters  $r_1$  and  $r_2$ , we use  $x_{\text{eff}}$  and  $v_{\text{eff}}$  as the primary parameters and determine  $r_1$  and  $r_2$  from Eqs. (93) and (94). Accordingly, the vertical axes in Plates 3–9 show the values of the effective size parameter, while the effective



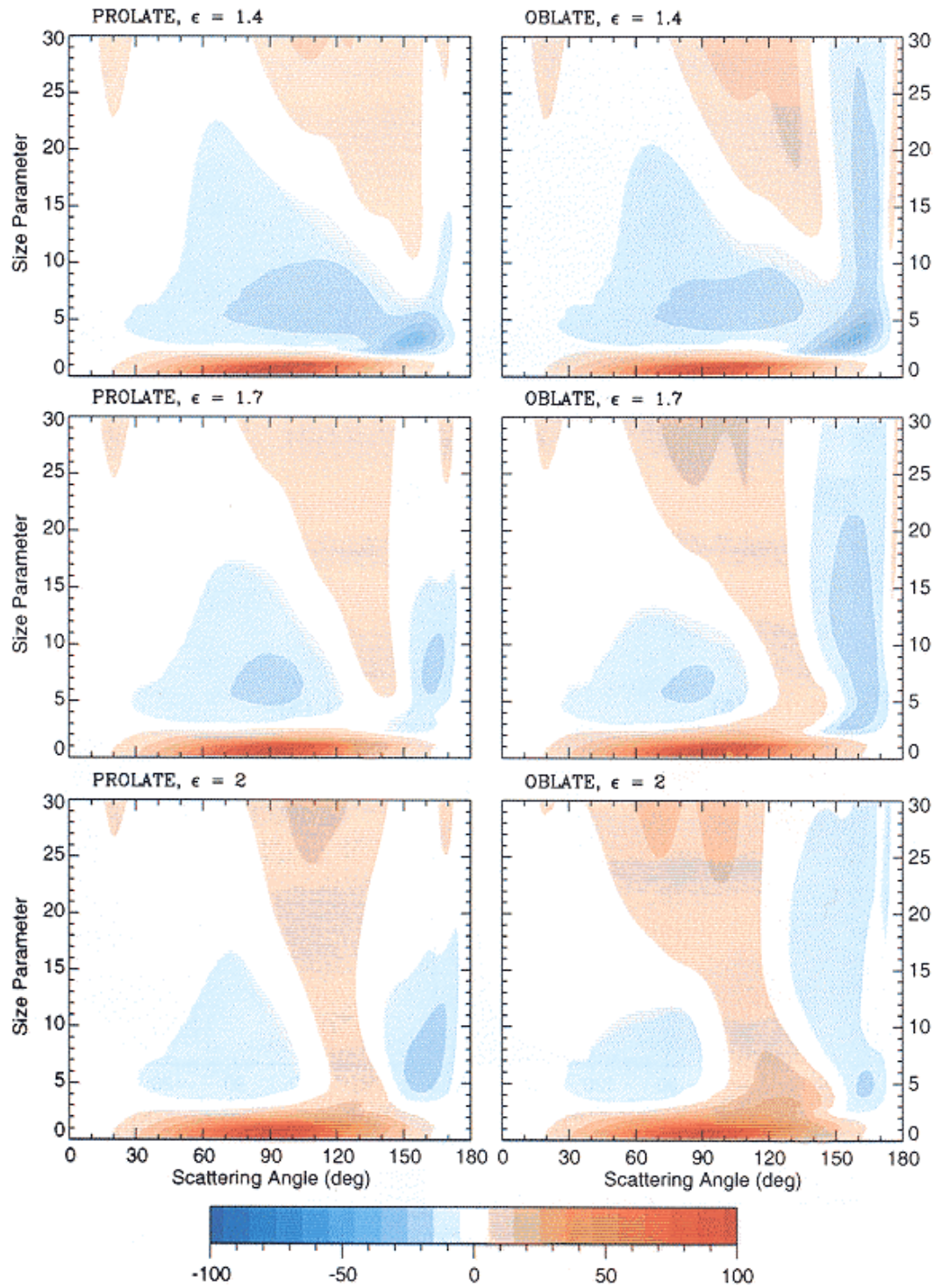


Plate 3. Degree of linear polarization vs scattering angle and effective size parameter for randomly oriented polydisperse spheroids.